Earth and Planetary Science Letters 480 (2017) 121–132

Contents lists available at ScienceDirect

Earth and Planetary Science Letters

www.elsevier.com/locate/epsl

# The neodymium stable isotope composition of the silicate Earth and chondrites

Alex J. McCoy-West [a,*], Marc-Alban Millet [b], Kevin W. Burton [a]

[a] Department of Earth Sciences, Durham University, Elvet Hill, Durham DH1 3LE, UK
[b] School of Earth and Ocean Sciences, Cardiff University, Park Place, Cardiff CF10 3AT, UK

ARTICLE INFO

*Article history:*
Received 10 July 2017
Received in revised form 1 October 2017
Accepted 4 October 2017
Available online 2 November 2017
Editor: F. Moynier

*Keywords:*
Nd isotopes
sulfide
mass-dependent fractionation
chondrites
MORB

ABSTRACT

The non-chondritic neodymium (Nd) $^{142}Nd/^{144}Nd$ ratio of the silicate Earth potentially provides a key constraint on the accretion and early evolution of the Earth. Yet, it is debated whether this offset is due to the Earth being formed from material enriched in *s*-process Nd isotopes or results from an early differentiation process such as the segregation of a late sulfide matte during core formation, collisional erosion or a some combination of these processes. Neodymium stable isotopes are potentially sensitive to early sulfide segregation into Earth's core, a process that cannot be resolved using their radiogenic counterparts. This study presents the first comprehensive Nd stable isotope data for chondritic meteorites and terrestrial rocks. Stable Nd measurements were made using a double spike technique coupled with thermal ionisation mass spectrometry. All three of the major classes of chondritic meteorites, carbonaceous, enstatite and ordinary chondrites have broadly similar isotopic compositions allowing calculation of a chondritic mean of $\delta^{146/144}Nd = -0.025 \pm 0.025‰$ (±2 s.d.; $n = 39$). Enstatite chondrites yield the most uniform stable isotope composition ($\Delta^{146/144}Nd = 26$ ppm), with considerably more variability observed within ordinary ($\Delta^{146/144}Nd = 72$ ppm) and carbonaceous meteorites ($\Delta^{146/144}Nd = 143$ ppm). Terrestrial weathering, nucleosynthetic variations and parent body thermal metamorphism appear to have little measurable effect on $\delta^{146/144}Nd$ in chondrites. The small variations observed between ordinary chondrite groups most likely reflect inherited compositional differences between parent bodies, with the larger variations observed in carbonaceous chondrites being linked to varying modal proportions of calcium–aluminium rich inclusions. The terrestrial samples analysed here include rocks ranging from basaltic to rhyolitic in composition, MORB glasses and residual mantle lithologies. All of these terrestrial rocks possess a broadly similar Nd isotope composition giving an average composition for the bulk silicate Earth of $\delta^{146/144}Nd = -0.022 \pm 0.034‰$ ($n = 30$). In the samples here magmatic differentiation appears to only have an effect on stable Nd in highly evolved magmas with heavier $\delta^{146/144}Nd$ values observed in samples with >70 wt% $SiO_2$. The average stable Nd isotope composition of chondrites and the bulk silicate Earth are indistinguishable at the 95% confidence level. However, mantle samples do possess variable stable Nd isotope compositions ($\Delta^{146/144}Nd = 75$ ppm) with an average $\delta^{146/144}Nd$ value of −0.008‰. If these heavier values represent the true composition of pristine mantle then it is not possible to completely rule out some role for core formation in accounting for some of the offset between the mantle and chondrites. Overall, these results indicate that the mismatch of $^{142}Nd$ between the Earth and chondrites is best explained by a higher proportion of *s*-process Nd in the Earth, rather than partitioning into sulfide or S-rich metal in the core.



## 1. Introduction

The planets of our Solar System are thought to have originated from the accumulation of dust and gas in the young Sun's protoplanetary disk, in which case the initial composition of the terrestrial planets should be similar to that of primitive 'chondritic' meteorites, fragments of material that escaped planetary differentiation. Although it has long been known that Earth's composition cannot be readily ascribed to any particular group of chondrites (e.g. Drake and Righter, 2002), the notion that the Earth has 'chondritic' refractory lithophile element ratios has persisted. The challenge to this assumption came from pioneering studies demonstrating that the $^{142}Nd/^{144}Nd$ isotope composition of chondritic meteorites is 18 ± 5 ppm lower than Earth's mantle

* Corresponding author.
*E-mail addresses:* a.j.mccoy-west@durham.ac.uk, alex.mccoywest@gmail.com (A.J. McCoy-West).

https://doi.org/10.1016/j.epsl.2017.10.004

(Boyet and Carlson, 2005; Carlson et al., 2007). The measured difference in $^{142}Nd/^{144}Nd$ requires the Sm/Nd ratio of the silicate Earth to be ~6% above the average chondritic value (known to within ±0.3%; Bouvier et al., 2008) providing definitive evidence that Earth's silicate mantle at the present day is non-chondritic. One potential explanation is that Earth's mantle may have experienced an early depletion event resulting in the formation of an incompatible element enriched reservoir with a low Sm/Nd ratio balancing that seen in the mantle at the present-day (Andreasen et al., 2008; Boyet and Carlson, 2005; Carlson et al., 2007). One possibility, is that this reservoir resides at the base of the mantle, in the seismically anomalous D″ layer overlying the core. Thus far, however, there is little chemical or thermal evidence for such a reservoir (Campbell and O'Neill, 2012). Moreover, because this reservoir must have been formed within the first ~30 Myr following accretion, while $^{146}Sm$ was extant, it has been argued that it would have been destroyed by the Giant-Impact that formed the Moon (Caro and Bourdon, 2010). Alternatively, it has been suggested that the Earth was initially assembled from chondritic material and was subsequently modified during planetary construction through the removal of its early silicate crust through, so-called, collisional erosion (O'Neill and Palme, 2008). Nevertheless, collisional erosion implies that the heat-producing elements are depleted up to 50% of their chondritic values, implying unlikely cooling rates for Earth over geological history (e.g. Campbell and O'Neill, 2012).

An alternative deep reservoir within the Earth is the metallic core, however, experimental data suggests that neither Sm nor Nd are partitioned into Fe–Ni metal at the conditions of core formation, nor is Nd preferentially incorporated over Sm (Bouhifd et al., 2015). Nevertheless, it has long been known that Earth's liquid outer core must be alloyed with ~10 wt.% 'light' elements (e.g. Birch, 1952) which may have been added late to the core during accretion. An oft cited candidate for that light element is sulfur (e.g. Boujibar et al., 2014; Labidi et al., 2013) and experimental data suggest that Sm and Nd, and other incompatible elements, may be substantially incorporated into sufide or sulfide-rich metal (Wohlers and Wood, 2015). In particular, Wohlers and Wood (2015) have shown that the partition coefficients of U, Nd and Sm are strong functions of the FeO content of silicate melts, increasing dramatically (with $D$ becoming >1) as the FeO content decreases below 1 wt.%. Furthermore, $D_{Nd}$ is always significantly greater than $D_{Sm}$ with $D_{Nd}/D_{Sm}$ approaching 1.5 in some cases. In this case, in a growing planet the segregation of a sulfide (or S-rich metal) from reduced FeO-poor silicate (conditions analogous to core formation) will lead to enrichment of the metallic phase in U and in Nd relative to Sm relative to the residual silicate mantle, providing a significant heat source to the core and a mantle with a superchondritic Sm/Nd ratio. If such a body represented Earth early in its history then the mantle would have developed a positive $^{142}Nd$ anomaly relative to chondrites (as observed) and much of the energy deficit identified for core convection (Labrosse et al., 2001) would be supplied by the additional U (and Th), while maintaining a chondritic complement of heat-producing elements for long-term heating of the Earth. This raises the possibility that Earth's missing refractory elements are simply located in a sulfide or sulfur-rich metal phase in the core, rather than being lost through collisional erosion or hidden in the deep mantle. However, this result has been questioned by more recent experimental work which indicates that there is little elemental fractionation between Sm and Nd at higher temperatures, closer to those that pertain to core formation (up to 2100 °C; Wohlers and Wood, 2017).

In parallel, recent high precision Nd and Sm isotope data indicate that, compared to chondrites, the Earth is enriched in Nd produced by the slow neutron capture process (*s*-process) of nucleosynthesis (Bouvier and Boyet, 2016; Burkhardt et al., 2016). This *s*-process excess leads to higher $^{142}Nd/^{144}Nd$ ratios, relative to chondrites. Therefore, the $^{142}Nd$ offset between the Earth and chondrites most likely reflects a higher proportion of *s*-process Nd in the Earth, rather than $^{146}Sm$ decay from a super-chondritic terrestrial reservoir (Bouvier and Boyet, 2016; Burkhardt et al., 2016; Saji et al., 2016). Nevertheless, the possibility remains that some part of the $^{142}Nd$ excess seen in the silicate Earth may be due to the presence of a hidden reservoir (up to 5 ± 2 ppm; Burkhardt et al., 2016). These different processes are not mutually exclusive and it is conceivable that the suprachondritic terrestrial $^{142}Nd/^{144}Nd$ is a consequence of some combination of nucleosynthetic processes, collisional erosion, and partitioning of Nd into the core.

If there is indeed a sulfide-rich reservoir in the deep Earth that has contributed to the $^{142}Nd$ discrepancy between chondrites and the terrestrial mantle, then Nd stable isotopes have the potential to trace this sulfide segregation event. Theory predicts that equilibrium stable isotope fractionation between silicate material (such as the mantle) and metal or sulfide (such as the core, depending on its S content) is driven by contrasts in bonding environment and oxidation state (e.g. Polyakov, 2009; Rustad and Yin, 2009). There is a significant contrast in bonding environment between sulfide and silicate, therefore heavy isotopes should be preferentially incorporated into high force-constant bonds involving rare earth element (REE) 3+ ions in silicate minerals. Preliminary measurements by Andreasen and Lapen (2015) indicate that mantle rocks may indeed possess heavier Nd isotope compositions than chondritic meteorites, consistent with the removal of light Nd into sulfide in the core, driving the residual mantle to heavier values. This study presents high-precision double spike stable Nd isotopic data for chondritic meteorites and terrestrial samples to assess the extent of fractionation between the silicate Earth and chondrites.

## 2. Samples and methods

### 2.1. Sample preparation and Nd separation

The samples investigated during this study include eleven carbonaceous chondrites (CI, CM, CO, CK, CV), seven enstatite chondrites (EH, EL) and fifteen ordinary chondrites (H, L, LL). For comparison a range of terrestrial materials were analysed and these include: twelve international rock standards that range from ultramafic to rhyolitic in composition; four optically pristine mid-ocean ridge basalt (MORB) glasses and four abyssal peridotites from the Garrett Fracture Zone, on the East Pacific Rise (Niu and Hékinian, 1997; Wendt et al., 1999); and two spinel lherzolite xenoliths from Kilbourne Hole, New Mexico (Burton et al., 1999; Jagoutz et al., 1980).

The majority of samples analysed herein were obtained as powders. When new powders where required samples were coarse crushed and unaltered chips, without visible fusion crust, were selected and then ultrasonically cleaned in distilled water and subsequently powdered using an agate mortar and pestle. Between 0.1 and 1 g of sample was taken to obtain between 100 and 200 ng of natural Nd and then spiked with our $^{145}Nd$–$^{150}Nd$ double spike, comprising 29% $^{145}Nd$ and 66% $^{150}Nd$, with an ideal sample to spike ratio of 60:40 based on the calculations given in Rudge et al. (2009; Fig. A1). Two digestion methods were employed during this study: 1) samples were placed in 15 mL Savillex beakers and dissolved using a concentrated HF–$HNO_3$ (3:1) mixture on a hotplate at ≥130 °C for 72 h; or 2) samples were placed in Carius tubes with a concentrated HCl–$HNO_3$ (5:4) mixture and sealed and heated at 220 °C for four days, following cooling all of the sample material was extracted and subsequently underwent a standard HF–$HNO_3$ dissolution to dissolve the silicate fraction. Carius tube digestions were implemented to ensure the complete digestion of samples containing refractory phases, such as the Cr-spinel present in some mantle samples (see Table ES1). Following dissolution the

samples were sequentially brought into solution in concentrated $HNO_3$ and HCl and refluxed on a hotplate for at least 24 h and dried down prior to being brought completely into solution in dilute HCl.

Neodymium was separated following well-established chromatographic techniques. The REE were separated from the sample matrix using polypropylene R1040 columns (2.5 mL resin capacity) filled with BioRad AG50W-x8 cation exchange resin. Samples were loaded in 2 mL of 1 M HCl, the matrix was then sequentially removed in 10 mL 1 M HCl + 1M HF, 12 mL 2.5 M HCl and 8 mL 2 M $HNO_3$ with the REE fraction collected in 14 mL of 6 M HCl. The REE fraction was then dried and Nd was separated from the other REE using polypropylene columns (internal diameter 88 × 4 mm) filled with Eichrom Ln-Spec resin. Samples were loaded in 0.5 mL of 0.2 M HCl, another 6 mL of 0.2 M HCl was then eluted, prior to the collection of Nd in the next 6 mL of 0.2 M HCl. This separation protocol results in virtually perfect separation of Sm (isobaric interferences on $^{144}$Nd, $^{148}$Nd, and $^{150}$Nd), however, residual Ce (isobaric interference on $^{142}$Nd) is present, and thus $^{142}$Nd/$^{144}$Nd ratios are not reported here. Total procedural blanks measured by isotope dilution with every batch of samples vary from 3–18 pg ($n = 6$) and in all cases were negligible. To confirm the chromatographic procedure had no effect on the stable Nd isotopic ratios repeat aliquots of the JNdi-1 standard were passed through the complete chemical procedure and the $\delta^{146}$Nd value obtained is indistinguishable within error from the unprocessed aliquots (Fig. A2).

### 2.2. Mass spectrometry and data reduction

Neodymium isotope measurements were performed using a Thermo-Fisher *TritonPlus* thermal ionisation mass spectrometer (TIMS) in the Arthur Holmes Geochemistry Labs at Durham University. In preparation for loading and TIMS analysis the solutions were evaporated to dryness and Nd samples individually loaded using 1 µL of 16 M $HNO_3$ onto Re ionisation filaments using a double filament assembly. Neodymium was measured as a metal ion in static collection mode using eight faraday cups using the following cup configuration: L4 = $^{142}$Nd; L3 = $^{143}$Nd; L2 = $^{144}$Nd; L1 = $^{145}$Nd; Ax = $^{146}$Nd; H1 = $^{147}$Sm; H2 = $^{148}$Nd; H3 = $^{150}$Nd. $^{147}$Sm was monitored and used to correct for isobaric interferences on $^{144}$Nd, $^{148}$Nd and $^{150}$Nd. Each analysis usually comprised 16–20 blocks of 20 scans. Stable Nd isotope ratios are expressed as $\delta^{146}$Nd which is the per mil deviation in the measured $^{146}$Nd/$^{144}$Nd relative to the widely measured Geological Survey of Japan Nd reference standard JNdi-1:

$$\delta^{146/144}\mathrm{Nd} = \left[\left(\frac{\frac{^{146}\mathrm{Nd}}{^{144}\mathrm{Nd}}\,\mathrm{Sample}}{\frac{^{146}\mathrm{Nd}}{^{144}\mathrm{Nd}}\,\mathrm{JNdi\text{-}1}}\right) - 1\right] \times 1000 \quad (1)$$

The double spike deconvolution used in this study is based on the algebraic resolution method used by Millet and Dauphas (2014). These calculations were confirmed using the Isospike deconvolution program of Creech and Paul (2015) which is based on the algebraic equations presented in Rudge et al. (2009), and the geometric iterative resolution method of Siebert et al. (2001), all three approaches yield identical results within analytical error (with a maximum offset ≤4 ppm). As the radiogenic isotope $^{143}$Nd is not used during double spike deconvolution, the spike proportion, and the geological and analytical fractionation factors resolved during deconvolution can be used to calculate the $^{143}$Nd/$^{144}$Nd ratios of the samples. Long-term reproducibility of 100–200 ng aliquots of the JNdi-1 standard throughout the period of analysis was $\delta^{146}$Nd = 0.003 ± 0.017‰ and $^{143}$Nd/$^{144}$Nd = 0.512100 ± 8 (±2$\sigma$; $n = 39$; Fig. A2). The external reproducibility of five digestions of the USGS rock standard BHVO-1 is $\delta^{146}$Nd = −0.029 ± 0.014‰ and $^{143}$Nd/$^{144}$Nd = 0.512972 ± 9 ($n = 11$), and four replicates of the Allende meteorite give $\delta^{146}$Nd = 0.057 ± 0.017‰ and $^{143}$Nd/$^{144}$Nd = 0.512525 ± 13. Taken together, these data suggest that the long-term reproducibility of the $\delta^{146}$Nd measurements is ±0.017‰ or better. Due to the novel nature of these measurements verifying the accuracy of our $\delta^{146}$Nd measurements is difficult. However, the $^{143}$Nd/$^{144}$Nd obtained herein following double spike deconvolution can be compared directly to previously published values for the same samples, with both techniques agreeing within analytical error (Fig. 1).

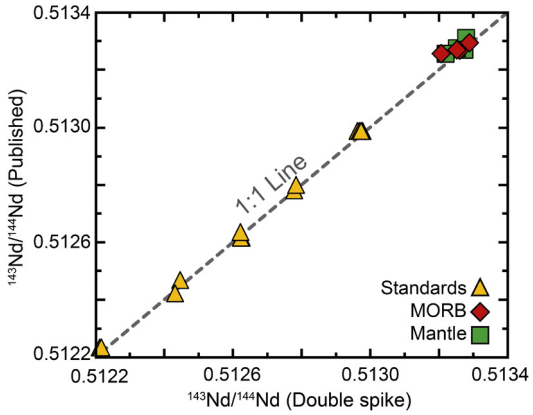


**Fig. 1.** Comparison of $^{143}$Nd/$^{144}$Nd isotope compositions generated here during double spike deconvolution, and published $^{143}$Nd/$^{144}$Nd data using conventional techniques. Published values come from Jochum et al. (2016) and Wendt et al. (1999).

## 3. Results

### 3.1. Neodymium in chondrites

A general increase in Nd concentration is observed across the different classes of chondritic meteorites from enstatite (0.42–0.61 ppm), to ordinary (0.58–0.85 ppm), to carbonaceous (0.84–1.08 ppm; Fig. 2a; Table 1), consistent with previously recognised trends regarding REE in chondrites (e.g. Nakamura, 1974). Two carbonaceous chondrites Orgueil and Cold Bokkeveld have significantly lower Nd concentrations (Nd = 0.58 and 0.46 ppm, respectively) than the other carbonaceous samples, and three desert finds Happy Canyon, Estacado and Maralinga (Nd = 0.98, 1.34 and 24.1 ppm, respectively) have significantly higher Nd than might be expected. The majority of the chondrites, irrespective of classification, fall within an extremely narrow range in radiogenic Nd isotope compositions with $^{143}$Nd/$^{144}$Nd varying from 0.5125 to 0.5128 ($n = 35$; Fig. 2b). Although, the three finds with higher than expected Nd concentrations also exhibit variable Nd isotope ratios ($^{143}$Nd/$^{144}$Nd: Maralinga = 0.5120; Happy Canyon = 0.5133; Estacado = 0.5153). The $\delta^{146/144}$Nd of our chondrite samples does not correlate with either $^{143}$Nd/$^{144}$Nd ratios or Nd concentration (Fig. 2).

Stable Nd isotope variations in chondrites range from $\delta^{146}$Nd −0.088‰ to 0.055‰ although the majority of the samples possess a significantly more restricted range of compositions (Fig. 3; Table 1). Of the samples analysed here, enstatite chondrites are the most homogeneous chondrite class ($\Delta^{146}$Nd = 26 ppm) with $\delta^{146}$Nd ranging from −0.039‰ to −0.013‰ and an average composition of $\delta^{146}$Nd = 0.023 ± 0.015‰ (±2$\sigma$; $n = 10$). Carbonaceous chondrites span the entire range of observed $\delta^{146}$Nd values in chondrites, and even within the CV3 group ($\Delta^{146}$Nd = 117 ppm) two well-characterised meteorites have distinctly different $\delta^{146}$Nd values (Vigarano = 0.029‰; Allende = −0.057‰; Table 1). The average composition of carbonaceous chondrites is

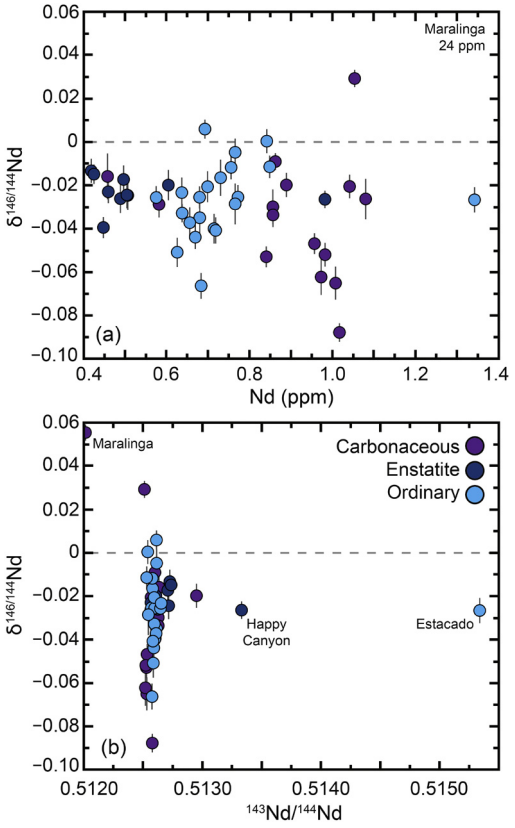


**Fig. 2.** Comparison of the Nd contents and isotopic compositions of the different classes of chondritic meteorites. Graphs of $\delta^{146}$Nd versus Nd concentration (a) and $^{143}$Nd/$^{144}$Nd (b), respectively.

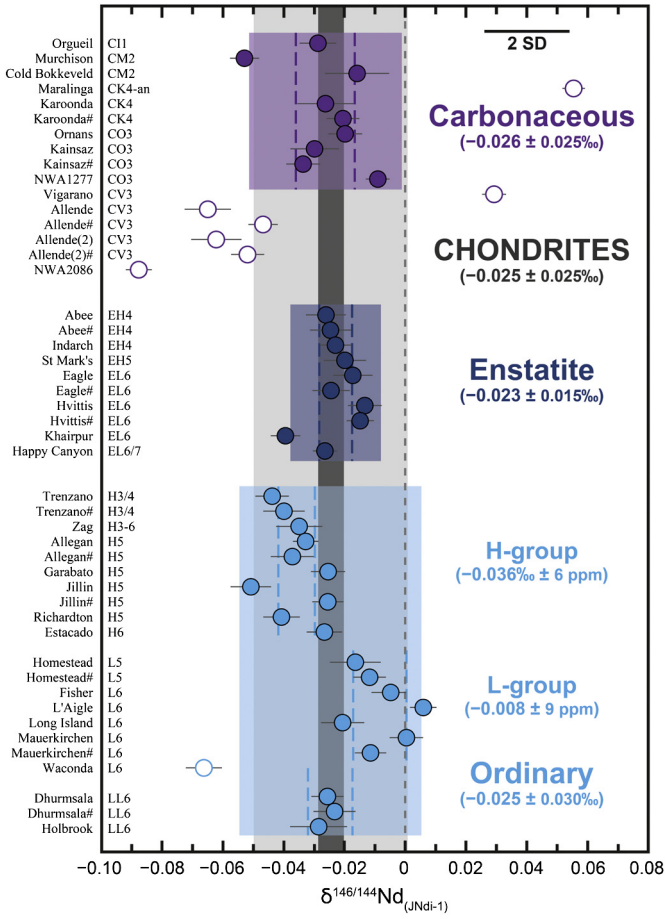


**Fig. 3.** Variation in $\delta^{146}$Nd in a selection of carbonaceous, enstatite and ordinary chondrites. The light grey shaded represents the chondritic average ±2 standard deviations (−0.025 ± 0.025‰; $n = 38$) with the dark grey band representing the 95% standard error of the mean (±0.004‰). The group CV3 carbonaceous chondrites and the find samples Maralinga and Waconda are excluded from the calculated averages (hollow symbols). For the different meteorite classes the shaded areas show ±2 standard deviations from the mean, with the dotted lines representing the 95% standard error of the mean. Individual analyses are shown with error bars representing their measured internal errors (±2 s.e.). The long term reproducibility (BHVO-1 = ±0.014‰ 2 SD; $n = 11$) of the measurements is shown by the black bar.

$\delta^{146}$Nd = −0.026 ± 0.025‰ ($n = 9$), excluding all of the CV3 meteorites and the desert find Maralinga. Ordinary H-group chondrites ($\delta^{146}$Nd = −0.051‰ to −0.025‰) appear to be systematically lighter than the L-group chondrites ($\delta^{146}$Nd = −0.021‰ to 0.006‰; Fig. 3), excluding the desert find Waconda which is significantly offset ($\Delta^{146}$Nd = 58 ppm) from the other L-group samples. The average composition of all ordinary chondrites is $\delta^{146}$Nd = −0.025 ± 0.030‰ ($n = 20$; excluding Waconda). All three major classes of chondrites (carbonaceous, enstatite and ordinary) have mean $\delta^{146}$Nd values that are within error at the 95% confidence level (Table 1), therefore it is possible to calculate an overall chondritic average of $\delta^{146}$Nd = −0.025 ± 0.025‰ ($n = 39$; 95% s.e. = ±0.004‰).

### 3.2. Stable Nd in terrestrial materials

A range of international rock standards that includes intrusive and extrusive rocks, that vary from basaltic to dacitic in composition, show limited stable Nd isotope variability with $\delta^{146}$Nd ranging from −0.046‰ to −0.011‰ ($\Delta^{146}$Nd = 35 ppm; Fig. 4; Table 2). Two samples, however, with rhyolitic bulk compositions display systematically heavier $\delta^{146}$Nd compositions with increasing $SiO_2$ (RGM-1 = −0.008‰; JG-2 = 0.013‰; Fig. 5a). The average composition of the terrestrial magmatic rock standards is $\delta^{146}$Nd = −0.029 ± 0.013‰ ($n = 18$, excluding the two samples with $SiO_2$ > 70 wt%). Four MORB glasses from the Garrett Fracture Zone show comparable $\delta^{146}$Nd to the standards with values ranging from −0.030‰ to −0.007‰ and a slightly heavier average composition of $\delta^{146}$Nd = −0.019 ± 0.019‰ ($n = 4$). While they are comparatively uniform in their major element compositions, mantle samples possess significantly more variable stable Nd ($\Delta^{146}$Nd = 75 ppm; Fig. 5b) than the other terrestrial rocks measured here, with $\delta^{146}$Nd ranging from −0.044‰ to 0.031‰. A significant degree of variability is even observed within a single lithology at the same location, with serpentinised harzburgites from the Garrett Fracture Zone ($\Delta^{146}$Nd = 48 ppm) and spinel lherzolites from Kilbourne Hole ($\Delta^{146}$Nd = 46 ppm) showing large resolvable differences. Although highly variable, an average composition for the mantle based on these analyses can be calculated as $\delta^{146}$Nd = −0.008 ± 0.053‰ ($n = 8$; 95% s.e. = ±0.022‰). Terrestrial reservoirs have broadly similar Nd isotopic compositions allowing an average composition of the bulk silicate Earth to be calculated with $\delta^{146}$Nd = −0.022 ± 0.034‰ ($n = 30$; 95% s.e. = ±0.006‰; Fig. 4).

## 4. Discussion

### 4.1. Previous stable Nd isotope measurements

Stable Nd isotope geochemistry is in its infancy with only a few published measurements of mass-dependent Nd isotopic variations (Ma et al., 2013; Saji et al., 2016; Wakaki and Tanaka, 2012). Wakaki and Tanaka (2012) used a double spike TIMS method to analyse 10 high-purity Nd oxide solutions and demonstrated variations of up to 0.3‰ in $\delta^{146}$Nd. Ma et al. (2013) measured a range

**Table 1**
Neodymium concentrations and isotopic compositions of chondritic meteorites.

| Sample | Classification | Fall/find | Nd (ppm) | $^{143}Nd/^{144}Nd$ | $\delta^{146/144}Nd$ | 2 s.d. | *n* |
|---|---|---|---|---|---|---|---|
| *Carbonaceous chondrites* | | | | | | | |
| Orgueil | CI1 | Fall | 0.582 | 0.512596 ± 3 | −0.029 ± 0.006 | | |
| Murchison | CM2 | Fall | 0.841 | 0.512527 ± 3 | −0.053 ± 0.005 | | |
| Cold Bokkeveld | CM2 | Fall | 0.458 | 0.512633 ± 6 | −0.016 ± 0.011 | | |
| Maralinga ∼ | CK4-an | Find | 24.17 | 0.512012 ± 2 | 0.055 ± 0.004 | | |
| Karoonda | CK4 | Fall | 1.080 | 0.512564 ± 5 | −0.026 ± 0.009 | | |
| Karoonda# | CK4 | | 1.041 | 0.512566 ± 3 | −0.021 ± 0.005 | | |
| Ornans | CO3 | Fall | 0.889 | 0.512949 ± 3 | −0.020 ± 0.006 | | |
| Kainsaz | CO3 | Fall | 0.856 | 0.512627 ± 5 | −0.030 ± 0.008 | | |
| Kainsaz# | CO3 | | 0.857 | 0.512626 ± 3 | −0.034 ± 0.006 | | |
| NWA1277 | CO3 | Find | 0.862 | 0.512598 ± 2 | −0.009 ± 0.004 | | |
| Vigarano ∼ | CV3 | Fall | 1.054 | 0.512510 ± 2 | 0.029 ± 0.004 | | |
| Allende ∼ | CV3 | Fall | 1.008 | 0.512530 ± 4 | −0.065 ± 0.008 | | |
| Allende# ∼ | CV3 | | 0.957 | 0.512531 ± 3 | −0.047 ± 0.005 | | |
| Allende(2) ∼ | CV3 | | 0.973 | 0.512518 ± 5 | −0.062 ± 0.008 | | |
| Allende(2)# ∼ | CV3 | | 0.982 | 0.512521 ± 3 | −0.052 ± 0.005 | | |
| NWA2086 ∼ | CV3 | Find | 1.017 | 0.512576 ± 2 | −0.088 ± 0.004 | | |
| | | | | **Average-Carbonaceous:** | **−0.026 ± 0.010** | **±0.025** | *9* |
| *Enstatite chondrites* | | | | | | | |
| Abee | EH4 | Fall | 0.489 | 0.512623 ± 4 | −0.026 ± 0.007 | | |
| Abee# | EH4 | | 0.507 | 0.512630 ± 4 | −0.025 ± 0.007 | | |
| Indarch | EH4 | Fall | 0.460 | 0.512566 ± 3 | −0.023 ± 0.005 | | |
| St Mark's | EH5 | Fall | 0.605 | 0.512605 ± 4 | −0.020 ± 0.007 | | |
| Eagle | EL6 | Fall | 0.497 | 0.512707 ± 4 | −0.017 ± 0.006 | | |
| Eagle# | EL6 | | 0.505 | 0.512714 ± 4 | −0.024 ± 0.006 | | |
| Hvittis | EL6 | Fall | 0.419 | 0.512723 ± 3 | −0.013 ± 0.006 | | |
| Hvittis# | EL6 | | 0.425 | 0.512734 ± 3 | −0.015 ± 0.005 | | |
| Khairpur | EL6 | Fall | 0.448 | 0.512600 ± 3 | −0.039 ± 0.005 | | |
| Happy Canyon | EL6/7 | Find | 0.982 | 0.513329 ± 3 | −0.026 ± 0.004 | | |
| | | | | **Average-Enstatite:** | **−0.023 ± 0.005** | **±0.015** | *10* |
| *Ordinary chondrites* | | | | | | | |
| Trenzano | H3/4 | Fall | 0.670 | 0.512589 ± 3 | −0.044 ± 0.005 | | |
| Trenzano# | H3/4 | | 0.715 | 0.512597 ± 4 | −0.040 ± 0.007 | | |
| Zag | H3-6 | Fall | 0.680 | 0.512612 ± 4 | −0.035 ± 0.008 | | |
| Allegan | H5 | Fall | 0.638 | 0.512593 ± 2 | −0.033 ± 0.004 | | |
| Allegan# | H5 | | 0.656 | 0.512607 ± 4 | −0.037 ± 0.007 | | |
| Garabato | H5 | Find | 0.772 | 0.512569 ± 3 | −0.025 ± 0.006 | | |
| Jillin | H5 | Fall | 0.626 | 0.512585 ± 3 | −0.051 ± 0.007 | | |
| Jillin# | H5 | | 0.680 | 0.512596 ± 3 | −0.026 ± 0.005 | | |
| Richardton | H5 | Fall | 0.719 | 0.512581 ± 3 | −0.041 ± 0.006 | | |
| Estacado | H6 | Find | 1.343 | 0.515338 ± 3 | −0.027 ± 0.006 | | |
| | | | | **Average-H group:** | **−0.036 ± 0.006** | **±0.017** | *10* |
| Homestead | L5 | Fall | 0.731 | 0.512578 ± 5 | −0.016 ± 0.008 | | |
| Homestead# | L5 | | 0.756 | 0.512576 ± 3 | −0.012 ± 0.005 | | |
| Fisher | L6 | Fall | 0.766 | 0.512612 ± 4 | −0.005 ± 0.006 | | |
| L'Aigle | L6 | Fall | 0.693 | 0.512611 ± 2 | 0.006 ± 0.004 | | |
| Long Island | L6 | Find | 0.699 | 0.512592 ± 4 | −0.021 ± 0.007 | | |
| Mauerkirchen | L6 | Fall | 0.842 | 0.512537 ± 3 | 0.000 ± 0.006 | | |
| Mauerkirchen# | L6 | | 0.849 | 0.512529 ± 3 | −0.011 ± 0.005 | | |
| Waconda ∼ | L6 | Find | 0.684 | 0.512574 ± 4 | −0.066 ± 0.006 | | |
| | | | | **Average-L group:** | **−0.008 ± 0.009** | **±0.019** | *7* |
| Dhurmsala | LL6 | Fall | 0.575 | 0.512644 ± 3 | −0.026 ± 0.005 | | |
| Dhurmsala# | LL6 | | 0.637 | 0.512650 ± 4 | −0.023 ± 0.007 | | |
| Holbrook | LL6 | Fall | 0.765 | 0.512542 ± 2 | −0.029 ± 0.009 | | |
| | | | | **Average-Ordinary:** | **−0.025 ± 0.007** | **±0.030** | *20* |
| | | | | **CHONDRITE AVERAGE:** | **−0.025 ± 0.004** | **±0.025** | *39* |

Errors on measured $^{143}Nd/^{144}Nd$ and $\delta^{146/144}Nd$ are 2 standard errors. To represent population uncertainty, both the two standard deviation (2 s.d.) and 95% standard errors (95% s.e. $= t * \text{s.d.}/(n)^{1/2}$, where $t =$ inverse survival function of the Student's t-test at the 95% significance level and $(n-1)$ degrees of freedom) are presented for averages. () Numbers in parentheses represent a separate digestion. # represents an independently spiked aliquot of the same digestion processed through the entire chemical procedure. ∼ denotes samples that are exclude from average calculations. The following samples are on loan from the Field Museum of Natural History, Chicago: Orgueil (ME 5503 #3), Murchison (ME 2644 #28.25), Indarch (ME 1404 #30), St Mark's (ME 3306 #3), Khairpur (ME 1538 #9) and Happy Cannyon (ME 2760 #4).

of terrestrial rock standards using a multi-collector inductively coupled plasma mass spectrometry (MC-ICP-MS) standard sample bracketing technique. Significant mass dependent variations can be artificially induced during column chromatography (Wakaki and Tanaka, 2012; showed $\delta^{146}Nd$ of seven fractions varied from 0.46‰ at the begin to −0.94‰ at the end of Nd collection) consequently it is imperative to obtain 100% yield when not using a double spike. The values reported by Ma et al. (2013) are often resolvably lighter (outside analytical error) than the double spike TIMS measurements for the same samples reported here (Fig. A3), this may result from an incomplete yield during chemical separation with heavy Nd isotopes being lost during Ce removal (see Fig. 1 in Ma et al., 2013) driving the residue to lighter values (as observed), thus we suggest that these data should be considered with caution. Most recently, Saji et al. (2016) used a MC-ICP-MS technique but developed an automated chromatographic procedure using a double-sized Ln-spec column and claim better than 99.5% Nd recovery effectively eliminating problems related to fraction-

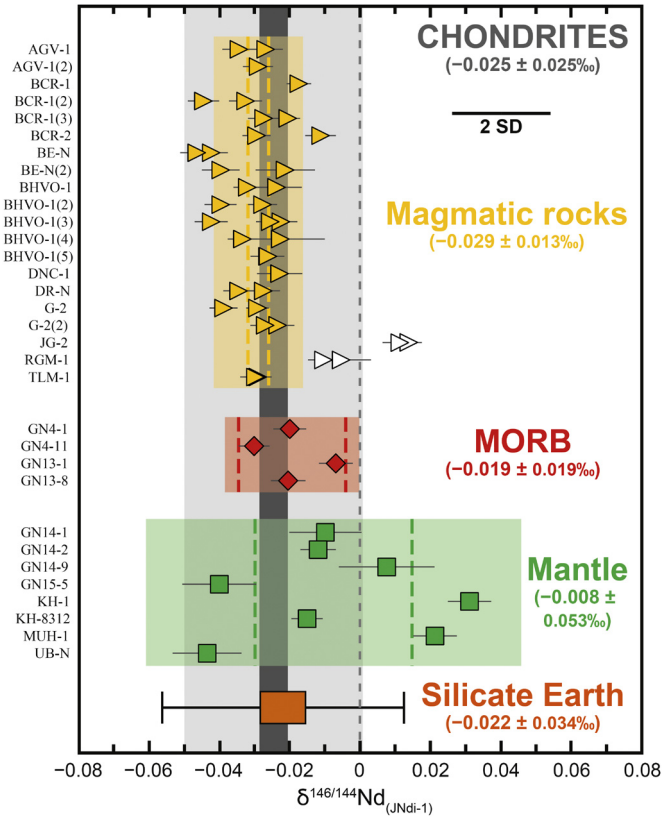


**Fig. 4.** Variation in $\delta^{146}$Nd in a selection of terrestrial rocks. The grey bars represent the average chondritic composition from Fig. 3. The shaded areas for the different groups show ±2 standard deviations from the mean, with the dotted lines representing the 95% standard error of the mean. Two high $SiO_2$ samples (JG-2 and RGM-1; hollow symbols) are excluded from the calculated means. To limit bias in the calculated means for the magmatic rock standards and bulk silicate Earth, they were calculated using the averages of any samples that were analysed on multiple occasions. Individual analyses are shown with error bars representing their measured internal errors (±2 s.e.). The long term reproducibility (BHVO-1 = ±0.014‰ 2 SD; $n = 11$) of the measurements is shown by the black bar.

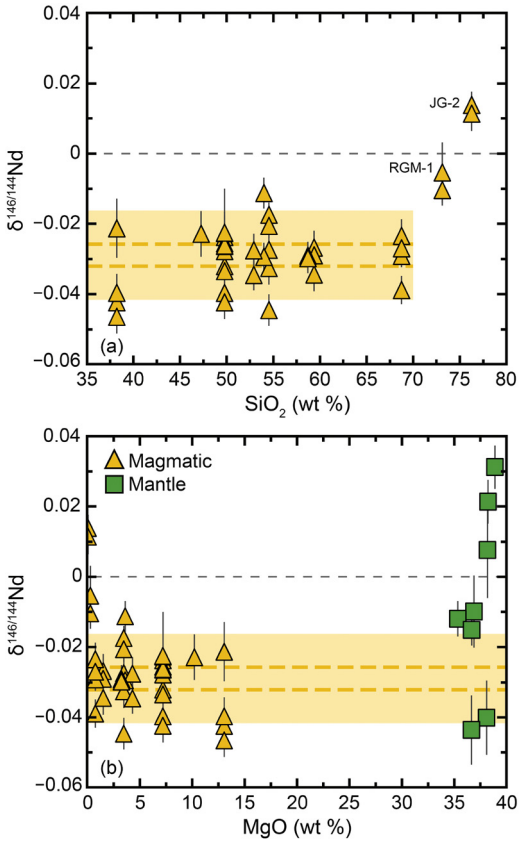


**Fig. 5.** Graphs showing the variability of $\delta^{146}$Nd in terrestrial magmatic rocks versus $SiO_2$ (a) and MgO (b) contents, respectively. The shaded area represents the average composition of the rock standards ±2 standard deviations from the mean (−0.029 ± 0.013‰; $n = 18$), with the dotted lines representing the 95% standard error of the mean (± 0.003‰). Samples with >70 wt% $SiO_2$ are excluded when calculating this mean. Major element compositions come from Burton et al. (1999), Jagoutz et al. (1979), Jochum et al. (2016) and Niu and Hékinian (1997).

ation during chemistry. They present results in $\varepsilon^{145}$Nd of 3 rock standards (BCR-2, BHVO-2 and GSP-2) and the Allende meteorite and conclude these materials are the same within analytical error (Fig. A3). These measurements are clumped averages of 10 mass spectrometry analyses from 5 different aliquots of the same digestion processed through chemistry ($n = 50$), with 95% confidence intervals varying from 8 to 31 ppm. The average compositions of 5 different aliquots from the same digestion of BCR-2 are highly variable with $\Delta^{146}$Nd = 60 ppm (Fig. A3). It is impossible to verify if the large variability in $\delta^{146}$Nd seen in different aliquots of the same digestion of homogeneous rock standards is an artefact from the chemical separation or simply a reflection of the true precision of plasma source technique of Saji et al. (2016). Using the double spike-TIMS technique implemented here 11 measurements of 5 digestions of the rock standard BHVO-1 have a 95% s.e. of 5 ppm and a $\Delta^{146}$Nd of 19 ppm. By comparison, using the average of averages approach implemented in Saji et al. (2016), the $\Delta^{146}$Nd obtained here is just 7 ppm with the external reproducibility ($\pm 2\sigma$) falling to just 6 ppm. Taken together, these results indicate that the isotope measurements of $\delta^{146}$Nd obtained using the double spike TIMS technique here provides data of the best accuracy and precision currently available.

### 4.2. Neodymium isotope variability in chondritic meteorites

The three major classes of chondritic meteorites all have mean $\delta^{146}$Nd values within error of each other at the 95% confidence level (95% s.e.) allowing the calculation of an overall chondritic average of $\delta^{146}$Nd = −0.025 ± 0.025‰. However, there are still significant variations amongst the analysed meteorites ($\Delta^{146}$Nd = 143 ppm), especially the carbonaceous chondrites. This variability could be the result of a number of different factors including: 1) terrestrial weathering; 2) inherited nucleosynthetic anomalies; 3) differences in thermal and alteration histories; 4) variable proportions of calcium–aluminium rich inclusions; and 5) inherited compositional differences between parent bodies.

#### 4.2.1. Terrestrial weathering

The majority of meteorites analysed here are observed falls, with eight samples being hot desert finds (Table 1: Estacado, Gabarato, Happy Canyon, Long Island, Maralinga, NWA1277, NWA2086 and Waconda), though all of the samples may have been subjected to some degree of terrestrial weathering. Exposure to a range of potential weathering agents including water, oxygen-rich air, salts and wind may have modified the original $\delta^{146}$Nd composition of some of the chondrites. Through analyses of fragments of the Holbrook meteorite collected in the Arizona desert over a 56 year period, Gibson and Bogard (1978) showed that Rb and Sr increased at least two-fold during weathering. Al-Kathiri et al. (2005) analysed up to 50 ka old meteorites collected from the Omani desert and observed a significant increases in Sr and Ba contents during troilite weathering, while pyroxene and olivine remained visibly unaltered in this weathering environment. Significant increases in Sr and Ba concentrations (up to 244 and 300 ppm, respectively; see Table ES3) are observed in both fall

**Table 2**
Neodymium concentrations and isotopic compositions of terrestrial materials.

| Sample | Rock type | Nd (ppm) | $^{143}Nd/^{144}Nd$ | $\delta^{146/144}Nd$ | 2 s.d. | *n* |
|---|---|---|---|---|---|---|
| *Magmatic rock standards* | | | | | | |
| AGV-1 | andesite | 33.02 | 0.512779 ± 3 | −0.034 ± 0.005 | | |
| AGV-1* | | 33.02 | 0.512775 ± 3 | −0.027 ± 0.005 | | |
| AGV-1(2) | andesite | 36.51 | 0.512777 ± 2 | −0.029 ± 0.004 | | |
| BCR-1 | basalt | 33.26 | 0.512625 ± 2 | −0.017 ± 0.003 | | |
| BCR-1(2) | basalt | 33.25 | 0.512624 ± 3 | −0.033 ± 0.005 | | |
| BCR-1(2)* | | 33.25 | 0.512619 ± 3 | −0.045 ± 0.004 | | |
| BCR-1(3) | basalt | 33.22 | 0.512623 ± 2 | −0.021 ± 0.004 | | |
| BCR-1(3)* | | 33.22 | 0.512621 ± 2 | −0.027 ± 0.004 | | |
| BCR-2 | basalt | 33.17 | 0.512621 ± 2 | −0.011 ± 0.004 | | |
| BCR-2* | | 33.17 | 0.512625 ± 2 | −0.029 ± 0.004 | | |
| BE-N | basalt | 78.52 | 0.512864 ± 3 | −0.042 ± 0.005 | | |
| BE-N* | | 78.52 | 0.512866 ± 3 | −0.046 ± 0.005 | | |
| BE-N(2) | basalt | 76.13 | 0.512863 ± 4 | −0.021 ± 0.008 | | |
| BE-N(2)* | | 76.13 | 0.512865 ± 3 | −0.021 ± 0.005 | | |
| BE-N(2)* | | 76.13 | 0.512864 ± 3 | −0.040 ± 0.005 | | |
| BHVO-1 | basalt | 28.66 | 0.512963 ± 4 | −0.024 ± 0.007 | | |
| BHVO-1* | | 28.66 | 0.512969 ± 2 | −0.032 ± 0.004 | | |
| BHVO-1(2) | basalt | 27.42 | 0.512974 ± 3 | −0.028 ± 0.004 | | |
| BHVO-1(2)* | | 27.42 | 0.512971 ± 3 | −0.040 ± 0.005 | | |
| BHVO-1(3) | basalt | 28.46 | 0.512968 ± 3 | −0.023 ± 0.005 | | |
| BHVO-1(3)* | | 28.47 | 0.512975 ± 2 | −0.026 ± 0.004 | | |
| BHVO-1(3)* | | 28.49 | 0.512970 ± 3 | −0.042 ± 0.005 | | |
| BHVO-1(4) | basalt | 28.67 | 0.512978 ± 3 | −0.023 ± 0.013 | | |
| BHVO-1(4)* | | 28.67 | 0.512974 ± 2 | −0.033 ± 0.004 | | |
| BHVO-1(5) | basalt | 29.12 | 0.512974 ± 3 | −0.026 ± 0.005 | | |
| BHVO-1(5)* | | 29.12 | 0.512978 ± 2 | −0.026 ± 0.004 | | |
| DNC-1 | dolerite | 5.69 | 0.512446 ± 4 | −0.023 ± 0.006 | | |
| DR-N | diorite | 27.05 | 0.512431 ± 3 | −0.028 ± 0.005 | | |
| DR-N* | | 27.03 | 0.512436 ± 2 | −0.035 ± 0.004 | | |
| G-2 | granite | 60.71 | 0.512211 ± 2 | −0.029 ± 0.003 | | |
| G-2* | | 60.71 | 0.512218 ± 2 | −0.039 ± 0.004 | | |
| G-2(2) | granite | 60.62 | 0.512216 ± 3 | −0.023 ± 0.005 | | |
| G-2(2)* | | 60.62 | 0.512217 ± 2 | −0.027 ± 0.004 | | |
| JG-2 ∼ | granite | 26.92 | 0.512218 ± 2 | 0.014 ± 0.004 | | |
| JG-2* ∼ | | 26.92 | 0.512220 ± 3 | 0.011 ± 0.005 | | |
| RGM-1 ∼ | rhyolite | 22.15 | 0.512784 ± 2 | −0.010 ± 0.004 | | |
| RGM-1* ∼ | | 22.15 | 0.512787 ± 2 | −0.005 ± 0.009 | | |
| TLM-1 | tonalite | 19.18 | 0.512616 ± 3 | −0.029 ± 0.004 | | |
| TLM-1* | | 19.18 | 0.512615 ± 3 | −0.030 ± 0.004 | | |
| | | | **Average-Magmatic:** | **−0.029 ± 0.003** | **±0.013** | *18* |
| *MORBs* | | | | | | |
| GN4-1 | glass | 4.10 | 0.513261 ± 3 | −0.020 ± 0.005 | | |
| GN4-11 | glass | 4.81 | 0.513253 ± 2 | −0.030 ± 0.004 | | |
| GN13-1 | glass | 5.24 | 0.513289 ± 3 | −0.007 ± 0.005 | | |
| GN13-8 | glass | 10.80 | 0.513207 ± 3 | −0.020 ± 0.005 | | |
| | | | **Average-MORB:** | **−0.019 ± 0.015** | **±0.019** | *4* |
| *Mantle* | | | | | | |
| GN14-1 | harzburgite | 0.742 | 0.513274 ± 3 | −0.010 ± 0.010 | | |
| GN14-2 | harzburgite | 0.163 | 0.513249 ± 3 | −0.012 ± 0.005 | | |
| GN14-9 | harzburgite | 0.115 | 0.513217 ± 5 | 0.008 ± 0.014 | | |
| GN15-5 | harzburgite | 0.262 | 0.513275 ± 3 | −0.040 ± 0.011 | | |
| KH-1 | lherzolite | 0.592 | 0.513241 ± 5 | 0.031 ± 0.006 | | |
| KH-8312 | lherzolite | 0.946 | 0.512990 ± 2 | −0.015 ± 0.004 | | |
| MUH-1 | harzburgite | 0.197 | 0.512963 ± 3 | 0.021 ± 0.006 | | |
| UB-N | serpentinite | 0.491 | 0.512918 ± 3 | −0.044 ± 0.010 | | |
| | | | **Average-Mantle:** | **−0.008 ± 0.022** | **±0.053** | *8* |
| | | | **SILICATE EARTH AVERAGE:** | **−0.022 ± 0.006** | **±0.034** | *30* |

Errors on measured $^{143}Nd/^{144}Nd$ and $\delta^{146/144}Nd$ are 2 standard errors. To represent population uncertainty, both the two standard deviation (2 s.d.) and 95% standard errors are presented for averages. () Numbers in parentheses represent a separate digestion. ∗ represents a duplicate analysis on a different filament. ∼ denotes samples that are exclude from average calculations.

and find samples in the meteorite fractions analysed here (Fig. 6a). Due to the inherent heterogeneity seen between different classes of chondrites, conservatively samples with chondrite normalised ratios <1.5 are considered unaltered. This leaves 14 of the samples analysed here that may have experienced some degree of terrestrial modification, however, no systematic change in $\delta^{146}Nd$ is seen with increasing $Ba/Yb_{(N)}$ (Fig. 6b), suggesting that alteration does not measurably perturb stable Nd isotopic compositions. Three of the find samples (Maralinga, Happy Canyon and Estacado) have Nd concentrations higher than expected for their class of chondrite (Fig. 2a), similar to light-REE mobility observed by Crozaz et al. (2003) in chondrites in desert environments, and the perturbed radiogenic $^{143}Nd/^{144}Nd$ ratios of these samples (Fig. 2b). Only in one case (i.e. Maralinga $\delta^{146}Nd = 0.055‰$) could this be suggested to have driven the stable Nd isotopic composition away from the chondritic average (Fig. 5b) and this may well be a function of the

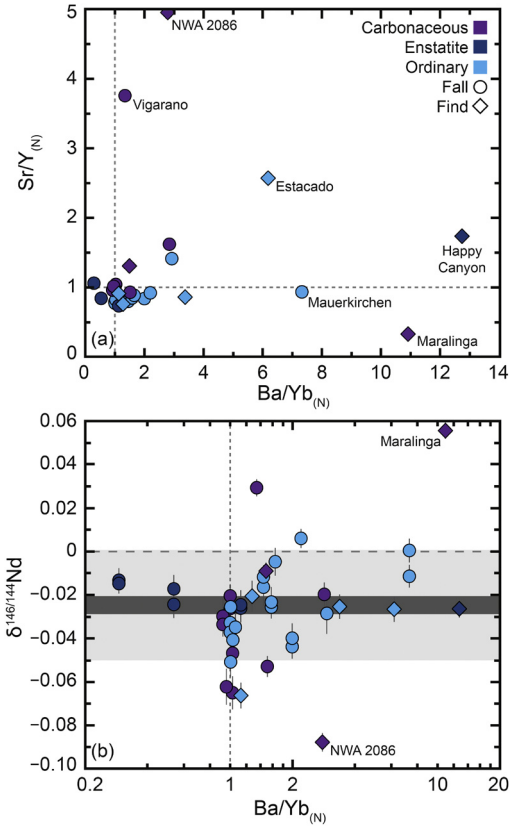


**Fig. 6.** The effect of terrestrial westering on the composition of chondritic meteorites. Observed fall (circles) and desert find (diamonds) samples are distinguished. (a) Graph of $Sr/Y_{(N)}$ versus $Ba/Yb_{(N)}$. Values are normalised using the CI chondrite composition in Palme and O'Neill (2014). Meteorites are considered unaltered if $Ba/Yb_{(N)}$ is $\leq$1.5. (b) Graph of $\delta^{146}$Nd versus $Ba/Yb_{(N)}$. The grey bars represents the average chondritic composition as in Fig. 3.

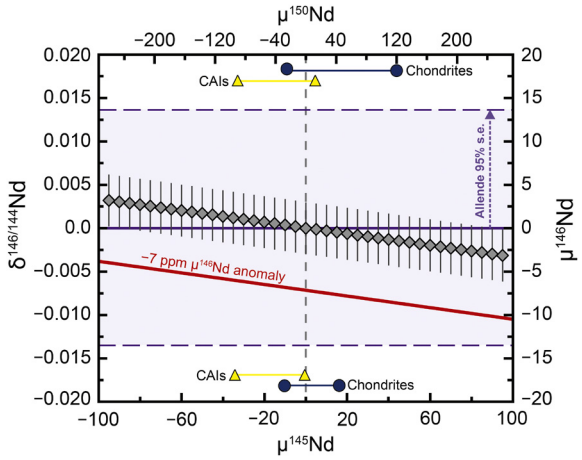


**Fig. 7.** Synthetic mixture model showing the effect of nucleosynthetic anomalies on $\delta^{146}$Nd ratios. A single model (diamonds) was developed as *s*-process nucleosynthetic anomalies on $^{145}$Nd and $^{150}$Nd are correlated based on the high-precision data of Burkhardt et al. (2016). The error bars on the individual points represent the smallest internal errors on any induvial analysis (±0.003‰). The dotted lines represent the 95% standard error on the mean of four replicates of the Allende meteorite (±0.014‰). The range of $\mu^{145}$Nd and $\mu^{150}$Nd anomalies measured in chondritic meteorites (circles) and calcium–aluminium rich inclusions (triangles) in the literature is also shown (Bouvier and Boyet, 2016; Brennecka et al., 2013; Burkhardt et al., 2016; Gannoun et al., 2011). Also shown (red line) is the effect of a −7 ppm anomaly on $^{146}$Nd as estimated for the Allende meteorite by Saji et al. (2016). (For interpretation of the references to colour in this figure legend, the reader is referred to the web version of this article.)

extreme enrichment of Nd in this meteorite (Nd = 24.1 ppm; Fig. A4). Overall, terrestrial weathering appears to have little resolvable effect on the $\delta^{146}$Nd value of chondrites.

### 4.2.2. Nucleosynthetic anomalies

Small variations in the distribution of *p*- and *s*-process radionuclides in the inner Solar System has produced measurable differences in the Nd isotopic compositions of the different classes of chondritic meteorites and the Earth (e.g. Andreasen and Sharma, 2006; Burkhardt et al., 2016; Gannoun et al., 2011). Therefore, it is important to assess any possible nucleosynthetic effects on the $\delta^{146}$Nd ratios reported here. Both of the isotopes used in the double spike ($^{145}$Nd and $^{150}$Nd) have observable nucleosynthetic anomalies. The high-precision dataset of Burkhardt et al. (2016) has shown that Nd nucleosynthetic variations are correlated ($\mu^{150}\text{Nd} = 2.74 \times \mu^{145}\text{Nd}$) resulting from the heterogeneous distribution of *s*-process radionuclides in the solar nebula. We have developed a simple model where a synthetic mixture of 60% JNdi-1, has its isotope composition modified with progressively larger anomalies on $^{145}$Nd and $^{150}$Nd, this was then mixed with 40% double spike and then deconvolved using the geometric iterative resolution method (Siebert et al., 2001) to assess the effects on $\delta^{146}$Nd (Fig. 7). In natural samples (bulk meteorites and calcium–aluminium rich inclusions) measured $\mu^{150}$Nd anomalies range from −91 to 120 (Bouvier and Boyet, 2016; Brennecka et al., 2013; Burkhardt et al., 2016; Gannoun et al., 2011), this level of anomaly results in variations in $\delta^{146}$Nd of $\leq \pm 1.5$ ppm, which is less than the smallest internal error on individual measurements (±3 ppm) and significantly less than the reproducibility of four replicates of the Allende meteorite (±14 ppm 95% s.e.; Fig. 7). Due to the convention of normalising to $^{146}$Nd/$^{144}$Nd to correct for instrumental mass bias during mass spectrometry, existing data for nucleosynthetic anomalies on $^{146}$Nd and $^{144}$Nd is sparse. By instead normalising to the $^{148}$Nd/$^{144}$Nd ratio, Saji et al. (2016) suggested that a $\mu^{146}$Nd anomaly of −6.3 ppm occurs in the Allende meteorite. The effect of a −7 ppm anomaly on $\mu^{146}$Nd results in the shift of $\delta^{146}$Nd to lighter values by the same magnitude (Fig. 7), although remaining well within the reproducibility of the stable Nd isotope data. In summary, nucleosynthetic anomalies may be responsible for minor fluctuations in $\delta^{146}$Nd values, but they cannot account for the range seen in chondrites.

### 4.2.3. Aqueous alteration and thermal metamorphism

Variations in the degree of aqueous alteration and/or thermal metamorphism that meteorites experience on their parent bodies may have perturbed their stable Nd isotopic compositions. For whole rock samples such a process requires open system behaviour, however, because of the small volumes of meteorite material used for analysis this may have occurred on a relatively small scale. Chondrites are classified according to their petrologic type and degree of alteration (Van Schmus and Wood, 1967), in this classification type 3.0 represents the most pristine material observed, with type 2 and 1 signifying more intense hydrous alteration. All of the seven recognised CI chondrites are of petrologic type 1 (Weisberg et al., 2006), indicating that they are heavily hydrated meteorites dominated by a fine-grained matrix with few primary chondrules or calcium aluminium-rich inclusions (CAIs). However, this level of intense aqueous alteration appears to have had little discernible effect on the isotopic composition of, for example, the meteorite Orgueil which possesses an $\delta^{146}$Nd value of −0.029‰ (Fig. 3), which is identical to the chondritic average. The majority of CM chondrites are of petrologic type 2 (Weisberg et al., 2006), although the degree of aqueous alteration experienced by different CM chondrites varies widely (Rubin et al., 2007). The meteorites analysed here include those considered both the least (Murchison) and most (Cold Bokkeveld) altered examples of CM2 meteorites (Browning et al., 1996). At

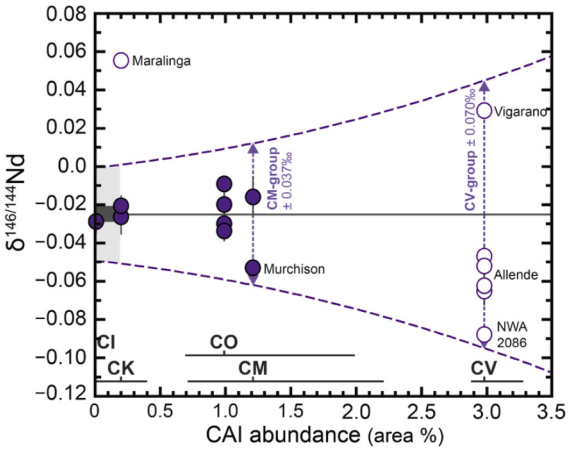


**Fig. 8.** Stable Nd isotope variations ($\delta^{146}$Nd) in carbonaceous chondrites relative to their modal abundance of calcium–aluminium rich inclusions in area %. Meteorites within a single group (e.g. CO = $0.99^{+1.0}_{-0.3}$) are all plotted at the calculated weighted average for that group (Hezel et al., 2008), with the $2\sigma$ errors on the CAI variability shown at the base of the graph. The grey bars represent the average chondritic composition from Fig. 3, plotted at <0.2% CAI content as this is maximum abundance observed in enstatite or ordinary chondrites (Hezel et al., 2008). The group CV3 carbonaceous chondrites and the anomalous find sample Maralinga are excluded from the chondritic average (hollow symbols). Calculated 2 s.e. errors on the CM- and CV-groups are ±0.037‰ and ±0.070‰, respectively, consistent with higher CAI contents resulting in increased variability in $\delta^{146}$Nd.

this stage it is not possible to definitively relate the difference in $\delta^{146}$Nd between these samples with the intensity of aqueous alteration. Petrologic type numbers rising from 3.1 to 6 designate increasing degrees of thermal metamorphism. Temperatures up to 900 °C are thought to be recorded in type 6 ordinary chondrites (Slater-Reynolds and McSween, 2005), during this heating the recrystallization of minerals combined with open system behaviour could, in principle, perturb their Nd stable isotopic compositions. Mineralogical evidence shows that 30–50% of the Nd in chondrites may be stored in phosphates, with the remainder distributed amongst the silicate phases, thus Nd is not easily mobilized during the early stages of metamorphism (Martin et al., 2013). Seven different group-H ordinary chondrites varying from petrologic type H3/4 to H6 have been analysed here with $\delta^{146}$Nd varying from −0.051‰ to −0.025‰ (Fig. 3). All H-group ordinary chondrites are indistinguishable from each other within the analytical uncertainties indicating there is no measurable variation in $\delta^{146}$Nd with increasing thermal metamorphism.

#### 4.2.4. Carbonaceous chondrites and the CAI effect

Carbonaceous chondrites span the entire range of $\delta^{146}$Nd values observed in chondritic meteorites ($\Delta^{146}$Nd = 143 ppm) and possess twice the variability of the other classes of chondritic meteorites. This additional variability may simply be the result of their unique constituents with carbonaceous chondrites containing variable proportions of chondrules, matrix and up to 6 wt% CAIs. Significant stable isotope whole rock variability in carbonaceous chondrites has also been observed for a range of other refractory lithophile elements (e.g. Eu: Moynier et al., 2006 or Sr: Charlier et al., 2012; Moynier et al., 2010). In carbonaceous meteorites CAIs host a significant proportion of the total Nd, a simple mass balance calculation using a range in CAI Nd concentration of 14–25 ppm (Burkhardt et al., 2016) and assuming 1 ppm Nd in the whole rock (see Table 1) and a modal CAI proportion of 3% (Hezel et al., 2008) shows that 42–75% of the Nd budget is controlled by CAIs. Therefore, the presence of significant Nd stable isotope anomalies in fine or coarse grained CAIs and the possible presence of fractionation and unknown nuclear (FUN) effect CAIs could cause the wider range in $\delta^{146}$Nd seen in carbonaceous chondrites. This preposition is supported by the progressively larger variability of $\delta^{146}$Nd seen in the different groups of carbonaceous chondrites as their modal CAI proportions increase (Fig. 8). Carbonaceous chondrites from the CI-, CK-, and CO-groups with <1% CAIs have relatively uniform $\delta^{146}$Nd, but as the proportion of CAIs continues to increases, 1.21% in the CM-group and 2.98% in the CV-group, the dispersion in $\delta^{146}$Nd also grows to ±0.037‰ and ±0.070‰, respectively. The exception to this observation is the anomalous CK4 Maralinga, a desert find that contains an extreme >20-fold enrichment of Nd (see Fig. A4) and has also been shown to have an abnormal Zn isotope composition (Pringle et al., 2017).

The CV (Vigarano-like) chondrites, possess a high proportion of matrix relative to chondrules and abundant large CAIs (weighted average 2.98%, but proportions up to 6% are observed; Hezel et al., 2008), isotopically they are the most variable group of carbonaceous chondrites ($\Delta^{146}$Nd = 119 ppm; Fig. 8). Two well-characterised meteorites have distinctly different $\delta^{146}$Nd values (Vigarano = 0.029‰; Allende = −0.057‰; Table 1) that diverge in opposite directions from the chondritic mean. For several other lithophile elements including, Ca (Niederer and Papanastassiou, 1984; Simon and DePaolo, 2010), Cd (Wombacher et al., 2008), Eu (Moynier et al., 2006), Sr (Charlier et al., 2012; Moynier et al., 2010; Patchett, 1980) and Zn (Luck et al., 2005), significant enrichments in the light isotopes have been measured in refractory CAIs relative to the meteorite matrix. These data are difficult to reconcile with condensation from a light isotope depleted gas (Richter, 2004), and rather have been attributed to kinetic effects (Richter, 2004) or electromagnetic separation (Moynier et al., 2006). Significantly, Charlier et al. (2012) showed for Sr that CAIs in Allende are isotopically light ($\delta^{88}$Sr = −0.07‰ to −0.35‰) and matrix material is heavy ($\delta^{88}$Sr = 0.65‰) with whole rock compositions simply reflecting a mixture of these components. By comparison, in Vigarano CAIs are significantly heavier ($\delta^{88}$Sr = 0.05‰) but so is the whole rock ($\delta^{88}$Sr = 0.35‰). If such an offset between CAIs, matrix and whole-rock also exists for stable Nd isotopes then this may go some way to explaining the heavier whole-rock value for Vigarano relative to Allende observed here.

The CV group has been further subdivided on the basis of petrologic characteristics into one reduced and two oxidised subgroups (Weisberg et al., 1997). Matrix/chondrule ratios increase in the order $CV_{red}$ (Vigarano-like = 0.5–0.6), $CV_{oxA}$ (Allende-like = 0.6–0.7)-$CV_{oxB}$ (Bali-like = 0.7–1.2), whereas metal/magnetite ratios decrease in the same order. A systematic decrease in $\delta^{146}$Nd values is observed as the meteorites become progressively more oxidised (e.g. Vigarano +0.029‰, Allende = −0.057‰, NWA 2086 = −0.088‰; this sample is a Bali-like CV on the basis of the chondrule proportion reported in Kereszturi et al., 2014). Mineralogical studies suggest that the differences between the sub-groups are a consequence of varying degrees of late-stage alteration (Krot et al., 1995). Stable Nd isotopes may therefore provide a means to trace aqueous alteration and oxidation in CV group meteorites although the mechanism by which this would occur remains poorly constrained.

#### 4.2.5. Inherited compositional differences between parent bodies

Each chondrite group is considered to have sampled a separate parent body (Weisberg et al., 2006). In this case it is possible that variable $\delta^{146}$Nd isotope compositions could be inherited from differences in the distribution of Nd in the protoplanetary disk or through the different mechanisms of formation of each these bodies. Ordinary chondrites, are thought to be derived from at least three separate parent bodies (H, L, and LL) on the basis of their major element chemistry, oxygen isotopic compositions and degree of iron oxidation (Yomogida and Matsui, 1984). Significant variability is seen within the ordinary chondrites analysed here, with H-group samples ($\delta^{146}$Nd = −0.051‰ to −0.025‰) appearing to

be systematically lighter than the L-group chondrites ($\delta^{146}$Nd = −0.021‰ to 0.006‰; Table 1). Although the average $\delta^{146}$Nd values of these two groups are indistinguishable at the $\pm 2\sigma$ level, with H-group ordinaries having $\delta^{146}$Nd = −0.036 ± 0.017‰ ($n = 10$; 95% s.e = ±0.006‰) and L-group ordinaries $\delta^{146}$Nd = −0.008 ± 0.019‰ ($n = 9$; 95% s.e. = ±0.009‰), their means are clearly resolvable at the 95% confidence level (Fig. 3). Systematic variations in the Ni, Zn and Cu stable isotope compositions of the different ordinary chondrites groups (from H to L and LL) have been documented and linked to evaporative processes or differences in parent body formation (Moynier et al., 2007). These systematic differences are not observed in $\delta^{146}$Nd. Experimental data indicates that Nd is not strongly partitioned into metal (Bouhifd et al., 2015), and is highly refractory (Lodders, 2003), and hence Nd isotopes are unlikely to be affected by metallic segregation or evaporation processes (i.e. volatile loss). Moynier et al. (2007) attribute variations in Cu isotopes amongst ordinary chondrites to the loss of sulfide, either during evaporation or removal to a metallic core. If light Nd is indeed preferentially partitioned into sulfide, then such a process could explain these variations, however, this is difficult to reconcile with the stable Nd isotope data given that it would fail to explain the lighter values in H-group chondrites than the chondritic mean (Fig. 3) and the fact that different groups of ordinary chondrite possess indistinguishable S contents (Cripe and Moore, 1975; Dreibus et al., 1995). In summary, the small difference in $\delta^{146}$Nd between H and L ordinary chondrites observed here are difficult to reconcile with planetary differentiation processes, instead it could simply be a heterogeneity that survives from the earliest stages of nebular condensation.

### 4.3. Modification of stable Nd isotopes during magmatic processes

Magmatic rocks can experience a number of processes including partial melting, fractional crystallisation, mixing and crustal assimilation each of which may have modified their Nd stable isotopic compositions.

#### 4.3.1. Magmatic differentiation

The rock standards analysed here are sourced from widely dispersed localities and a range of intrusive and extrusive rock types including basalt, andesite, dolerite, diorite, granite, rhyolite and tonalite (Table 2; Fig. A5). Samples with basaltic to dacitic major element compositions show minimal stable Nd isotope variability ($\Delta^{146}$Nd = 35 ppm), with an average composition of $\delta^{146}$Nd = −0.030 ± 0.014‰, and no systematic changes with magmatic differentiation ($SiO_2$ = 38–69 wt%; Fig. 5a). In contrast, the two most felsic rock standards analysed possess progressively heavier $\delta^{146}$Nd as $SiO_2$ increases above 70 wt% (RGM-1: $SiO_2$ = 73 wt%; $\delta^{146}$Nd = −0.008‰ and JG-2: $SiO_2$ = 76 wt%; $\delta^{146}$Nd = 0.013‰). One cause of this enrichment in heavy Nd in the rhyolitic samples could be the crystallisation of accessory mineral phases. Sphene, allanite and apatite can all show 100–1000 fold enrichments of light REE relative to whole-rock (e.g. Sawka, 1988) and such partitioning might induce an isotopic fractionation due to a contrast in bonding coordination with the melt. This data suggests that in highly evolved rocks, magmatic processes may modify their stable Nd isotopic composition although the exact cause remains unknown.

#### 4.3.2. Partial melting

Neodymium behaves as an incompatible element during mantle melting. Therefore, mass balance dictates that, if any stable isotope fractionation were to occur during this process, it should be recorded in the residue, whereas the original Nd stable isotopic composition of the mantle source will be transferred to the product of melting. Simple peritectic melt modelling (McCoy-West et al., 2015) demonstrates that with just 10% melting >80% of the original Nd budget, in both the spinel and garnet facies mantle (92% and 84%, respectively; Fig. A6), would be in the melt fraction. The broadly similar Nd isotope compositions of basaltic samples measured here suggests that the mantle preserves a homogeneous $\delta^{146}$Nd composition. In addition, that 6 out of the 8 mantle samples analysed here yield values that are within error of the basaltic samples indicates that little fractionation occurs during partial melting (Fig. 4). This is further highlighted by comparing MORB glasses and their complementary abyssal peridotites from the Garrett Fracture Zone. The MORB glasses have $\delta^{146}$Nd values ranging from −0.030‰ to −0.007‰ and an average composition of −0.019‰ ($n = 4$), the abyssal peridotites (mantle residues) have slightly more variable $\delta^{146}$Nd with values ranging from −0.040‰ to 0.008‰ and an average of −0.014‰. For the samples measured here, at least, there is no resolvable effect on $\delta^{146}$Nd that can be attributed to partial melting.

### 4.4. Planetary differentiation and fractionation of stable Nd isotopes

#### 4.4.1. Removal of light Nd to the core during planetary formation?

Recent experimental work suggests that the outer core may contain a significant amount of sulfide added during the final stages of accretion (Wade et al., 2012), and that at reduced conditions analogous to core formation sulfide can incorporate a substantial quantities of refractory lithophile and heat-producing elements (e.g. Nd and U; Wohlers and Wood, 2015). Therefore a substantial amount of Nd may have been separated into a sulfide or a sulfur-rich metal phase during the final stages of planetary differentiation, possibly providing a mechanism to resolve the $^{142}$Nd mismatch between chondritic meteorites and the Earth. Neodymium stable isotopes have the potential to provide a tracer of sulfide segregation, because there is a significant contrast in bonding environment between sulfide and silicate, where heavy isotopes should be preferentially incorporated into the high force-constant bonds involving $REE^{3+}$ ions in silicate minerals (i.e. mantle). At first sight, however, based on the stable Nd data presented here it seems unlikely that a significant amount Nd could have been sequestered into the core or else REE incorporation into sulfide in the core was not accompanied by stable Nd isotope fractionation. The average $^{146}$Nd/$^{144}$Nd isotope composition of chondrites ($\delta^{146}$Nd = −0.025 ± 0.004‰) is indistinguishable from that of the bulk silicate Earth ($\delta^{146}$Nd = −0.022 ± 0.006‰) at the 95% confidence level (Fig. 4). This result is consistent with recent high precision Nd and Sm isotopic data that suggest, rather, that a heterogeneous distribution of *s*-process radionuclides in the Solar Nebula is responsible for the $^{142}$Nd discrepancy between chondrites and the Earth (Bouvier and Boyet, 2016; Burkhardt et al., 2016). Although a small fraction (~5 ppm) of the original $^{142}$Nd anomaly between the Earth and enstatite chondrites remains unaccounted for Burkhardt et al. (2016).

The mantle samples analysed here display significantly more variability in $\delta^{146}$Nd than the other terrestrial reservoirs measured ($\Delta^{146}$Nd = 75 ppm; Table 2), and on average ($\delta^{146}$Nd = −0.008‰) are slightly heavier than the chondritic meteorites. An analysis of variance test shows that the mantle samples possess a resolvably different population to both the chondritic meteorites and the terrestrial rock standards at the 99% significance level (p-value <0.001), whereas the rock standards and chondrites are statistically the same. This small difference (17 ppm) between mantle samples and chondrites is consistent with two possible interpretations: 1) the peridotites are indeed heavier and Nd could have been fractionated during the sequestration of light Nd into the core; or 2) the crustal magmatic rocks are more representative of the bulk Earth, due to the incompatible nature of Nd mass balance suggests that melts will dominate the Nd budget after c. 5% melting (Fig. A6). A number of processes may be responsible for

varying the $\delta^{146}$Nd of peridotites, these include partial melting, melt metasomatism, mineralogical variations, and serpentinisation or alteration during sample emplacement. Two ostensibly identical pristine spinel lherzolites from Kilbourne Hole having significantly different $\delta^{146}$Nd ($\Delta^{146}$Nd = 46 ppm). Until a more systematic study of mantle rocks is undertaken, to better understand the processes causing variability in $\delta^{146}$Nd, it is impossible to say definitively if the $\delta^{146}$Nd of the mantle was indeed perturbed due to core formation or some other secondary process.

## 5. Conclusions

Here we present the first comprehensive Nd stable isotope data for chondritic meteorites and a range of terrestrial rocks using a double spike TIMS methodology.

The major classes of chondritic meteorites, carbonaceous, enstatite and ordinary chondrites all have broadly similar isotopic compositions allowing the calculation of an overall chondritic mean of $\delta^{146}$Nd = $-0.025 \pm 0.025$‰. Enstatite chondrites yield the most uniform stable isotope composition ($\Delta^{146}$Nd = 26 ppm), with considerably more variability observed within ordinary ($\Delta^{146}$Nd = 72 ppm) and carbonaceous meteorites ($\Delta^{146}$Nd = 143 ppm). The effects of terrestrial weathering, nucleosynthetic anomalies and parent body metamorphism produce no resolvable variations on the $\delta^{146}$Nd of chondrites. A resolvable offset ($\Delta^{146}$Nd = 28 ppm) between H and L group ordinary chondrites is probably the result of an inherited heterogeneity from the earliest stages of condensation preserved in their different parent bodies. The larger variations observed in carbonaceous chondrites, specifically the CM- and CV-groups correspond to varying modal proportions of calcium–aluminium rich inclusions.

The terrestrial samples analysed here include rocks ranging from basaltic to rhyolitic in composition, MORB glasses and mantle restites. All of these terrestrial reservoirs possess a broadly similar Nd isotope compositions allowing the calculation of a mean for the bulk silicate Earth composition of $\delta^{146}$Nd = $-0.022 \pm 0.034$‰. Magmatic differentiation appears to have minimal effect on the $\delta^{146}$Nd of basaltic to dactitic magmas, with resolvably heavier $\delta^{146}$Nd values only observed in highly evolved magmas with >70 wt% $SiO_2$.

The average $\delta^{146}$Nd of chondrites and the silicate Earth are indistinguishable at the 95% confidence level. Mantle samples possess highly variable stable Nd isotope compositions ($\Delta^{146}$Nd = 75 ppm) with an average $\delta^{146}$Nd of $-0.008$‰, if these heavier values represent the true composition of the mantle then it is not possible to completely rule out some contribution from core formation in the offset between the mantle and chondrites. Although, due its highly incompatible behaviour Nd mass balance suggest that melting products strongly dominant the Nd budget. Thus on balance, these results are consistent with the $^{142}$Nd mismatch between the Earth and chondrites being best explained by a higher proportion of *s*-process Nd in the Earth, rather than partitioning into sulfide or S-rich metal in the core.

## Acknowledgements

Geoff Nowell, in particular, is thanked for his generous help and insightful discussions over the last few years. We thank Chris Ottley for assistance with ICP-MS analysis. We are grateful to the Field Museum of Natural History, Chicago for the loan of six of the meteorite samples to MAM. Frederic Moynier, Greg Brennecka and an anonymous reviewer are thanked for are thanked for their constructive comments which greatly improved the manuscript. This project was funded by the NERC grant NE/N003926/1 to KWB.

## Appendix A. Supplementary material

Supplementary material related to this article can be found online at https://doi.org/10.1016/j.epsl.2017.10.004.

## References

Al-Kathiri, A., Hofmann, B.A., Jull, A.J.T., Gnos, E., 2005. Weathering of meteorites from Oman: correlation of chemical and mineralogical weathering proxies with $^{14}$C terrestrial ages and the influence of soil chemistry. Meteorit. Planet. Sci. 40, 1215–1239.

Andreasen, R., Lapen, T.J., 2015. Mass-dependent neodymium isotopic variations in planetary materials – determined using a neodymium double spike. In: Lunar & Planetary Science Conference, p. 2847.

Andreasen, R., Sharma, M., 2006. Solar nebula heterogeneity in p-process samarium and neodymium isotopes. Science 314, 806.

Andreasen, R., Sharma, M., Subbarao, K.V., Viladkar, S.G., 2008. Where on Earth is the enriched Hadean reservoir? Earth Planet. Sci. Lett. 266, 14–28.

Birch, F., 1952. Elasticity and constitution of the Earth's interior. J. Geophys. Res. 57, 227–286.

Bouhifd, M.A., Boyet, M., Cartier, C., Hammouda, T., Bolfan-Casanova, N., Devidal, J.L., Andrault, D., 2015. Superchondritic Sm/Nd ratio of the Earth: impact of Earth's core formation. Earth Planet. Sci. Lett. 413, 158–166.

Boujibar, A., Andrault, D., Bouhifd, M.A., Bolfan-Casanova, N., Devidal, J.-L., Trcera, N., 2014. Metal–silicate partitioning of sulphur, new experimental and thermodynamic constraints on planetary accretion. Earth Planet. Sci. Lett. 391, 42–54.

Bouvier, A., Boyet, M., 2016. Primitive Solar System materials and Earth share a common initial $^{142}$Nd abundance. Nature 537, 399–402.

Bouvier, A., Vervoort, J.D., Patchett, P.J., 2008. The Lu–Hf and Sm–Nd isotopic composition of CHUR: constraints from unequilibrated chondrites and implications for the bulk composition of terrestrial planets. Earth Planet. Sci. Lett. 273, 48–57.

Boyet, M., Carlson, R.W., 2005. $^{142}$Nd evidence for early (>4.53 Ga) global differentiation of the silicate Earth. Science 309, 576–581.

Brennecka, G.A., Borg, L.E., Wadhwa, M., 2013. Evidence for supernova injection into the solar nebula and the decoupling of r-process nucleosynthesis. Proc. Natl. Acad. Sci. USA 110, 17241–17246.

Browning, L.B., McSween, H.Y., Zolensky, M.E., 1996. Correlated alteration effects in CM carbonaceous chondrites. Geochim. Cosmochim. Acta 60, 2621–2633.

Burkhardt, C., Borg, L.E., Brennecka, G.A., Shollenberger, Q.R., Dauphas, N., Kleine, T., 2016. A nucleosynthetic origin for the Earth's anomalous $^{142}$Nd composition. Nature 537, 394–398.

Burton, K.W., Schiano, P., Birck, J.-L., Allègre, C.J., 1999. Osmium isotope disequilibrium between mantle minerals in a spinel-lherzolite. Earth Planet. Sci. Lett. 172, 311–322.

Campbell, I.H., O'Neill, H.S.C., 2012. Evidence against a chondritic Earth. Nature 483, 553–558.

Carlson, R.W., Boyet, M., Horan, M., 2007. Chondrite barium, neodymium, and samarium isotopic heterogeneity and Early Earth differentiation. Science 316, 1175–1178.

Caro, G., Bourdon, B., 2010. Non-chondritic Sm/Nd ratio in the terrestrial planets: consequences for the geochemical evolution of the mantle–crust system. Geochim. Cosmochim. Acta 74, 3333–3349.

Charlier, B.L.A., Nowell, G.M., Parkinson, I.J., Kelley, S.P., Pearson, D.G., Burton, K.W., 2012. High temperature strontium stable isotope behaviour in the early solar system and planetary bodies. Earth Planet. Sci. Lett. 329, 31–40.

Creech, J.B., Paul, B., 2015. IsoSpike: improved double-spike inversion software. Geostand. Geoanal. Res. 39, 7–15.

Cripe, J.D., Moore, C.B., 1975. Total sulfur content of ordinary chondrites. Meteoritics 10, 387.

Crozaz, G., Floss, C., Wadhwa, M., 2003. Chemical alteration and REE mobilization in meteorites from hot and cold deserts. Geochim. Cosmochim. Acta 67, 4727–4741.

Drake, M.J., Righter, K., 2002. Determining the composition of the Earth. Nature 416, 39–44.

Dreibus, G., Palme, H., Spettel, B., Zipfel, J., Wänke, H., 1995. Sulfur and selenium in chondritic meteorites. Meteoritics 30, 439–445.

Gannoun, A., Boyet, M., Rizo, H., El Goresy, A., 2011. $^{146}$Sm–$^{142}$Nd systematics measured in enstatite chondrites reveals a heterogeneous distribution of $^{142}$Nd in the solar nebula. Proc. Natl. Acad. Sci. USA 108, 7693–7697.

Gibson, E.K., Bogard, D.D., 1978. Chemical alterations of the Holbrook Chondrite resulting from terrestrial weathering. Meteoritics 13, 277–289.

Hezel, D.C., Russell, S.S., Ross, A.J., Kearsley, A.T., 2008. Modal abundances of CAIs: implications for bulk chondrite element abundances and fractionations. Meteorit. Planet. Sci. 43, 1879–1894.

Jagoutz, E., Carlson, R.W., Lugmair, G.W., 1980. Equilibrated Nd-unequilibrated Sr isotopes in mantle xenoliths. Nature 286, 708–710.

Jagoutz, E., Palme, H., Baddenhausen, H., Blum, K., Cendales, M., Dreibus, G., Spettel, B., Waenke, H., Lorenz, V., 1979. The abundances of major, minor and trace elements in the earth's mantle as derived from primitive ultramafic nodules. In:

Lunar and Planetary Science Conference, 10th. Pergamon Press, Inc., Houston, Texas, pp. 2031–2050.
Jochum, K.P., Weis, U., Schwager, B., Stoll, B., Wilson, S.A., Haug, G.H., Andreae, M.O., Enzweiler, J., 2016. Reference values following ISO guidelines for frequently requested rock reference materials. Geostand. Geoanal. Res. 40, 333–350.
Kereszturi, A., Blumberger, Z., Józsa, S., May, Z., Müller, A., Szabó, M., Tóth, M., 2014. Alteration processes in the CV chondrite parent body based on analysis of NWA 2086 meteorite. Meteorit. Planet. Sci. 49, 1350–1364.
Krot, A.N., Scott, E.R.D., Zolensky, M.E., 1995. Mineralogical and chemical modification of components in CV3 chondrites: nebular or asteroidal processing? Meteoritics 30, 748–775.
Labidi, J., Cartigny, P., Moreira, M., 2013. Non-chondritic sulphur isotope composition of the terrestrial mantle. Nature 501, 208–211.
Labrosse, S., Poirier, J.-P., Le Mouël, J.-L., 2001. The age of the inner core. Earth Planet. Sci. Lett. 190, 111–123.
Lodders, K., 2003. Solar System abundances and condensation temperatures of the elements. Astrophys. J. 591, 1220–1247.
Luck, J.-M., Othman, D.B., Albarède, F., 2005. Zn and Cu isotopic variations in chondrites and iron meteorites: early solar nebula reservoirs and parent-body processes. Geochim. Cosmochim. Acta 69, 5351–5363.
Ma, J., Wei, G., Liu, Y., Ren, Z., Xu, Y., Yang, Y., 2013. Precise measurement of stable neodymium isotopes of geological materials by using MC-ICP-MS. J. Anal. At. Spectrom. 28, 1926–1931.
Martin, C., Debaille, V., Lanari, P., Goderis, S., Vandendael, I., Vanhaecke, F., Vidal, O., Claeys, P., 2013. REE and Hf distribution among mineral phases in the CV–CK clan: a way to explain present-day Hf isotopic variations in chondrites. Geochim. Cosmochim. Acta 120, 496–513.
McCoy-West, A.J., Bennett, V.C., O'Neill, H.S.C., Hermann, J., Puchtel, I.S., 2015. The interplay between melting, refertilization and carbonatite metasomatism in off-cratonic lithospheric mantle under Zealandia: an integrated major, trace and platinum group element study. J. Petrol. 56, 563–604.
Millet, M.-A., Dauphas, N., 2014. Ultra-precise titanium stable isotope measurements by double-spike high resolution MC-ICP-MS. J. Anal. At. Spectrom. 29, 1444–1458.
Moynier, F., Agranier, A., Hezel, D.C., Bouvier, A., 2010. Sr stable isotope composition of Earth, the Moon, Mars, Vesta and meteorites. Earth Planet. Sci. Lett. 300, 359–366.
Moynier, F., Blichert-Toft, J., Telouk, P., Luck, J.-M., Albarède, F., 2007. Comparative stable isotope geochemistry of Ni, Cu, Zn, and Fe in chondrites and iron meteorites. Geochim. Cosmochim. Acta 71, 4365–4379.
Moynier, F., Bouvier, A., Blichert-Toft, J., Telouk, P., Gasperini, D., Albarède, F., 2006. Europium isotopic variations in Allende CAIs and the nature of mass-dependent fractionation in the solar nebula. Geochim. Cosmochim. Acta 70, 4287–4294.
Nakamura, N., 1974. Determination of REE, Ba, Fe, Mg, Na and K in carbonaceous and ordinary chondrites. Geochim. Cosmochim. Acta 38, 757–775.
Niederer, F.R., Papanastassiou, D.A., 1984. Ca isotopes in refractory inclusions. Geochim. Cosmochim. Acta 48, 1279–1293.
Niu, Y., Hékinian, R., 1997. Basaltic liquids and harzburgitic residues in the Garrett Transform: a case study at fast-spreading ridges. Earth Planet. Sci. Lett. 146, 243–258.
O'Neill, H.S.C., Palme, H., 2008. Collisional erosion and the non-chondritic composition of the terrestrial planets. Philos. Trans. R. Soc., Math. Phys. Eng. Sci. 366, 4205–4238.
Palme, H., O'Neill, H.S.C., 2014. 3.1 – Cosmochemical estimates of mantle composition. In: Holland, H.D., Turekian, K.K. (Eds.), Treatise on Geochemistry, second edition. Elsevier, Oxford, pp. 1–39.
Patchett, P.J., 1980. Sr isotopic fractionation in Ca–Al inclusions from the Allende meteorite. Nature 283, 438–441.
Polyakov, V.B., 2009. Equilibrium iron isotope fractionation at core–mantle boundary conditions. Science 323, 912–914.
Pringle, E.A., Moynier, F., Beck, P., Paniello, R., Hezel, D.C., 2017. The origin of volatile element depletion in early solar system material: clues from Zn isotopes in chondrules. Earth Planet. Sci. Lett. 468, 62–71.
Richter, F.M., 2004. Timescales determining the degree of kinetic isotope fractionation by evaporation and condensation. Geochim. Cosmochim. Acta 68, 4971–4992.
Rubin, A.E., Trigo-Rodríguez, J.M., Huber, H., Wasson, J.T., 2007. Progressive aqueous alteration of CM carbonaceous chondrites. Geochim. Cosmochim. Acta 71, 2361–2382.
Rudge, J.F., Reynolds, B.C., Bourdon, B., 2009. The double spike toolbox. Chem. Geol. 265, 420–431.
Rustad, J.R., Yin, Q.-Z., 2009. Iron isotope fractionation in the Earth's lower mantle. Nat. Geosci. 2, 514–518.
Saji, N.S., Wielandt, D., Paton, C., Bizzarro, M., 2016. Ultra-high-precision Nd-isotope measurements of geological materials by MC-ICPMS. J. Anal. At. Spectrom. 31, 1490–1504.
Sawka, W.N., 1988. REE and trace element variations in accessory minerals and hornblende from the strongly zoned McMurry Meadows Pluton, California. Earth Environ. Sci. Trans. R. Soc. Edinb. 79, 157–168.
Siebert, C., Nägler, T.F., Kramers, J.D., 2001. Determination of molybdenum isotope fractionation by double-spike multicollector inductively coupled plasma mass spectrometry. Geochem. Geophys. Geosyst. 2, 1032.
Simon, J.I., DePaolo, D.J., 2010. Stable calcium isotopic composition of meteorites and rocky planets. Earth Planet. Sci. Lett. 289, 457–466.
Slater-Reynolds, V., McSween, H.Y., 2005. Peak metamorphic temperatures in type 6 ordinary chondrites: an evaluation of pyroxene and plagioclase geothermometry. Meteorit. Planet. Sci. 40, 745–754.
Van Schmus, W.R., Wood, J.A., 1967. A chemical-petrologic classification for the chondritic meteorites. Geochim. Cosmochim. Acta 31, 747–765.
Wade, J., Wood, B.J., Tuff, J., 2012. Metal–silicate partitioning of Mo and W at high pressures and temperatures: evidence for late accretion of sulphur to the Earth. Geochim. Cosmochim. Acta 85, 58–74.
Wakaki, S., Tanaka, T., 2012. Stable isotope analysis of Nd by double spike thermal ionization mass spectrometry. Int. J. Mass Spectrom. 323–324, 45–54.
Weisberg, M.K., McCoy, T.J., Krot, A.N., 2006. Systematics and evaluation of meteorite classification. In: Lauretta, D.S., McSween, H.Y. (Eds.), Meteorites and the Early Solar System II. Univ. Ariz. Press, Tucson, pp. 19–52.
Weisberg, M.K., Prinz, M., Clayton, R.N., Mayeda, T.K., 1997. CV3 chondrites: three subgroups, not two (abstract). Meteorit. Planet. Sci. 32, 138–139.
Wendt, J.I., Regelous, M., Niu, Y., Hékinian, R., Collerson, K.D., 1999. Geochemistry of lavas from the Garrett Transform Fault: insights into mantle heterogeneity beneath the eastern Pacific. Earth Planet. Sci. Lett. 173, 271–284.
Wohlers, A., Wood, B.J., 2015. A mercury-like component of early Earth yields uranium in the core and high mantle $^{142}$Nd. Nature 520, 337–340.
Wohlers, A., Wood, B.J., 2017. Uranium, thorium and REE partitioning into sulfide liquids: implications for reduced S-rich bodies. Geochim. Cosmochim. Acta 205, 226–244.
Wombacher, F., Rehkämper, M., Mezger, K., Bischoff, A., Münker, C., 2008. Cadmium stable isotope cosmochemistry. Geochim. Cosmochim. Acta 72, 646–667.
Yomogida, K., Matsui, T., 1984. Multiple parent bodies of ordinary chondrites. Earth Planet. Sci. Lett. 68, 34–42.